EJN fens European Journal of Neuroscience

European Journal of Neuroscience, Vol. 31, pp. 238–249, 2010 doi:10.1111/j.1460-9568.2009.07049.x

SYNAPTIC MECHANISMS

Neural cell adhesion molecule is required for stability of reinnervated neuromuscular junctions

Peter H. Chipman,[1,*] Colin K. Franz,[1,*] Alexandra Nelson,[1] Melitta Schachner [2,3] and Victor F. Rafuse[1]
[1]Department of Anatomy and Neurobiology, Dalhousie University, Sir Charles Tupper Medical Building, 5850 College Street, Halifax, Nova Scotia, Canada, B3H 1X5
[2]Zentrum für Molekulare Neurobiologie, Universität Hamburg, Hamburg, Germany
[3]W.M. Keck Center for Collaborative Neuroscience and Department of Cell Biology and Neuroscience, Rutgers University, Piscataway, NJ, USA

Keywords: mouse, myopathy, neural cell adhesion molecule, neuromuscular junction, regeneration, synapse

Abstract

Studies examining the etiology of motoneuron diseases usually focus on motoneuron death as the defining pathophysiology of the disease. However, impaired neuromuscular transmission and synapse withdrawal often precede cell death, raising the possibility that abnormalities in synaptic function contribute to disease onset. Although little is known about the mechanisms maintaining the synaptic integrity of neuromuscular junctions (NMJs), *Drosophila* studies suggest that Fasciclin II plays an important role. Inspired by these studies we used a reinnervation model of synaptogenesis to analyze neuromuscular function in mice lacking neural cell adhesion molecule (NCAM), the Fasciclin II vertebrate homolog. Our results showed that the recovery of contractile force was the same in wild-type and NCAM−/− mice at 1 month after nerve injury, indicating that endplates were appropriately reformed. This normality was only transient because the contractile force and myofiber number decreased at 3 months after injury in NCAM−/− mice. Both declined further 3 months later. Myofibers degenerated, not because motoneurons died but because synapses were withdrawn. Although neurotransmission was initially normal at reinnervated NCAM−/− NMJs, it was significantly compromised 3 months later. Interestingly, the selective ablation of NCAM from motoneurons, or muscle fibers, did not mimic the deficits observed in reinnervated NCAM−/− mice. Taken together, these results indicate that NCAM is required to maintain normal synaptic function at reinnervated NMJs, although its loss pre-synaptically or post-synaptically is not sufficient to induce synaptic destabilization. Consideration is given to the role of NCAM in terminal Schwann cells for maintaining synaptic integrity and how NCAM dysfunction may contribute to motoneuron disorders.

Introduction

Progressive muscle weakness and wasting are defining symptoms associated with motoneuron diseases including amyotrophic lateral sclerosis (ALS) and spinal muscular atrophy. Although these symptoms are usually attributed to motoneuron death, it remains to be determined whether this accurately reflects the pathophysiology of the diseases. For example, abnormalities in synaptic function appear in patients with ALS prior to electrophysiological signs of motoneuron degeneration (Maselli *et al.*, 1993). Impaired neuromuscular transmission and synaptic withdrawal precede motoneuron death in animal models of motoneuron disease (Frey *et al.*, 2000; Kong *et al.*, 2009). Finally, a transgenic mouse model of familial ALS dies due to synapse withdrawal at the neuromuscular junction (NMJ) even when cell death is prevented by the genetic deletion of Bax (Gould *et al.*, 2006). Together, these studies indicate that the loss of synaptic integrity precedes, and may even precipitate, muscle weakness and motoneuron death in various motoneuron diseases (Conforti *et al.*, 2007). Unfortunately, the molecular mechanisms underlying the destabilization of NMJs in motoneuron disease are not known. This is, in part, because the cellular components responsible for synaptic stability are poorly understood.

Neural cell adhesion molecule (NCAM) is a candidate synaptic stability molecule because it is expressed on axons, terminal Schwann cells (tSCs) and myofibers during development (Nieke & Schachner, 1985; Covault & Sanes, 1986; Martini & Schachner, 1986; Rafuse & Landmesser, 2000). After nerve–muscle contact, NCAM is down-regulated along motor axons and muscle fibers in an activity-dependent manner (Rieger *et al.*, 1985; Covault & Sanes, 1986). However, even into adulthood, NCAM remains highly expressed in pre-synaptic terminals, at the base of junctional folds, in subsynaptic T-tubules and tSCs (Covault & Sanes, 1986). This continued expression suggests that NCAM regulates neuromuscular function after synaptic contact. Indeed, this is the case in *Drosophila* where its homolog, Fasciclin II (Harrelson & Goodman, 1988), is essential for maintaining NMJs during larval development (Schuster *et al.*, 1996). In its absence, *Drosophila* larvae die because motor axons withdraw from newly formed synapses. Although motor axons do not withdraw

Correspondence: Dr Victor F. Rafuse, as above.
E-mail: vrafuse@dal.ca

*P.H.C. and C.K.F. contributed equally to this work.

Received 1 September 2009, revised 28 October 2009, accepted 10 November 2009

in NCAM−/− mice, they do form smaller NMJs and exhibit neurotransmission deficits when stimulated at high frequencies (i.e. 200 Hz) (Rafuse *et al.*, 2000; Polo-Parada *et al.*, 2001).

The absence of axonal withdrawal in NCAM−/− mice indicates that NCAM is either not required for synaptic stability or that other gene products compensate for its loss during development (Moscoso *et al.*, 1998; Gu *et al.*, 2003). The present study was designed to address this issue using a reinnervation model of synaptogenesis. The rationale for this approach was based on the fact that many genes expressed during peripheral nerve development are not re-expressed after injury (Bosse *et al.*, 2006). Our results show that the recovery of contractile force was the same in wild-type and NCAM−/− mice at 1 month after nerve injury. This similarity was only transient, however, because many newly formed synapses were later eliminated in NCAM−/− mice. This elimination was concurrent with deficits in neurotransmitter release, withdrawal of motor axons and the presence of degenerating muscle fibers.

Materials and methods

Four different strains of male and female mice were used. Wild-type C57BL/6 mice (Charles River, Wilmington, MA, USA) and NCAM−/− mice, generated on a C57BL/6 background (Cremer *et al.*, 1994), were bred and housed locally. $NCAM^{flx/flx}$::$Hb9^{cre/+}$, which lack NCAM in motoneurons, were generated by breeding NCAM-floxed ($NCAM^{flx/flx}$) mice (Bukalo *et al.*, 2004) with mice expressing cre-recombinase under the control of the human homeobox gene 9 (Hb9) promoter (Yang *et al.*, 2001), whereas $NCAM^{flx/flx}$::$HSA^{cre/+}$ mice, which lack NCAM on muscle fibers, were generated by crossing $NCAM^{flx/flx}$ mice with mice expressing cre-recombinase under the control of the human α-skeletal actin (HSA) promoter (Miniou *et al.*, 1999; Cifuentes-Diaz *et al.*, 2001). Hb9 and HSA promoters are activated at embryonic day 12.5 and post-natal day 10, respectively (Cifuentes-Diaz *et al.*, 2001; Yang *et al.*, 2001). All procedures were conducted in accordance with the guidelines of the Canadian Council on Animal Care and the Dalhousie University Committee on Laboratory Animals.

Surgery

All surgeries were performed on 12-week-old adult mice unless otherwise noted. Animals were anesthetized with isoflurane (Baxter, Toronto, ON, Canada) and one of the two surgeries was performed under aseptic conditions. (i) A small incision was made in the skin above the knee in order to expose the tibial nerve. Using fine forceps, the tibial nerve was crushed twice consecutively 10 mm distal to its divergence from the sciatic nerve. Denervation was visually confirmed by noting muscle contraction and subsequent transparency of the nerve at the crush site. (ii) A small incision was made in the skin overlying the dorsal shank muscles. The soleus muscle was exposed and 0.5 μL of 1% cholera toxin subunit b conjugated to Alexa Fluor 594 (C22842; Invitrogen, Burlington, ON, Canada) was injected into the soleus muscle near the nerve entry point. All animals were provided with a subcutaneous injection of Anafen (5 mg/kg; Merial, Morgan Baie d'Urlé, Quebec, Canada) immediately following each surgery.

In-vitro *isometric tension and electromyogram recordings*

Mice were anaesthetized with isoflurane and killed by cervical dislocation and their right hindlimb was quickly dissected and placed into ice-cold, oxygenated Tyrode's solution(125 mM NaCl, 24 mM $NaHCO_3$, 5.37 mM KCl, 1 mM $MgCl_2$, 1.8 mM $CaCl_2$ and 5% dextrose). The soleus muscle and nerve supply were isolated and cut free at the insertion points on the femur and calcaneous bones. The proximal muscle tendon was securely pinned down on a Sylgard (Dow Corning, Midland, MI, USA)-coated recording chamber that was perfused with oxygenated Tyrode's solution maintained at 20–22°C. A suture (2-0) was tied to the distal tendon and connected to a force transducer (FT 03; Grass Technologies, West Warwick, RI, USA). A fine-tipped polyethylene stimulating suction electrode (PE-190; Clay Adams, Sparks, MD, USA) was used to deliver electrical current to the soleus nerve via an S88 stimulator (Grass Technologies) that was isolated from ground using a stimulus isolation unit (PSIU6; Grass Technologies). The electromyogram (EMG) was always recorded from the midbelly of the soleus muscle with a second polyethylene suction electrode and amplified with a bandwidth between 3 Hz and 10 kHz (EX4-400; Dagan Corporation, Minneapolis, MN, USA) as described by Rafuse *et al.* (2000). Monophasic electrical stimuli (0.01 ms) were used to elicit maximal isometric contractions and EMG responses were acquired at 10 kHz using a DIGIDATA 1322A A/D board and AXOSCOPE 9.2 software (Axon Instruments, Union City, CA, USA).

Intracellular muscle fiber electrophysiology

Intracellular muscle fiber recordings were performed from unoperated and reinnervated soleus muscle fibers in well-oxygenated Tyrode's solution (95% O_2 and 5% CO_2). To reduce the number of quanta released upon nerve stimulation, and thus prevent action potential responses in the myofibers, we used a low calcium Tyrode's solution containing 125 mM NaCl, 5.37 mM KCl, 24 mM $NaHCO_3$, 5 mM $MgCl_2$, 0.6 mM $CaCl_2$ and 5% dextrose (see also Everett & Ernst, 2004). Evoked responses were recorded by stimulating the soleus nerve at a rate of 0.5 Hz via a tight-fitting suction electrode connected to a Grass Technologies S88 stimulator with SIU5 stimulus isolation unit. Responses were recorded with a Duo 773 intracellular amplifier (WPI, New Haven, CT, USA) connected to a Dagan amplifier and digitized as described above. The micropipettes (resistances from 20 to 25 MO) that were used for recording were filled with 3 M KCl. Electrophysiological measurements were not recorded if the initial resting potential (−70 to −85 mV) decreased by 10% of its original value (Rafuse *et al.*, 2000). A failure was scored as a stimulus without a subsequent change in resting membrane potential (0 mV amplitude). The quantal content for each NMJ was calculated by the ratio of the mean endplate potential (EPP): mean miniature endplate potential (mEPP) amplitudes. At least 150 EPPs, and 40–80 mEPPs, were recorded per myofiber.

Immunofluorescence and histology

Immediately following the cessation of the physiological recordings, the muscles were pinned at their physiological length, immersed in a 1 : 2 mixture of 20% sucrose/phosphate-buffered saline (PBS) and optimal cutting temperature. compound and then rapidly frozen in isopentane cooled with dry ice. In some instances, the pinned muscles were fixed overnight in 4% paraformaldehyde/PBS for later endplate analysis (see below). Frozen muscles were sectioned at 30 μm on a cryostat, dried overnight, incubated with anti-slow myosin IgA primary antibody (1 : 10; S58; Developmental Studies Hybridoma Bank, Iowa City, IA, USA) overnight at 4°C and washed several times in PBS. Slides were post-fixed for 15 min in 4% paraformaldehyde/PBS, washed several times in PBS, incubated with anti-fast

myosin IgG primary antibody (1 : 500; M4276; Sigma Aldrich, Oakville, ON, Canada) at room temperature (21°C) for 1 h, washed several times in PBS, incubated with Alexa Fluor 546 goat anti-mouse IgG (1 : 500; A11003; Invitrogen) and fluorescein-conjugated goat anti-mouse IgA (1 : 500; 55492; Cappel, Aurora, OH, USA) secondary antibodies for 1 h at room temperature, washed several times in PBS, and finally mounted in a 50% glycerol/PBS mixture containing 0.03 mg/mL ρ-phenylenediamine to prevent fading. Sections were photographed with a digital camera (C4742; Hamamatsu Photonics, Hamamatsu, Japan) using IPLAB acquisition software (Version 4.0; BD Biosciences, Rockville, MD, USA).

For endplate morphology, fixed soleus muscles were teased into small bundles of muscle fibers, incubated in 0.1 M glycine for 1 h, washed in PBS and placed in rhodamine-conjugated α-bungarotoxin (α-btx) (1 : 100, Invitrogen) for 1–2 h at room temperature. After several washes in PBS, the fibers were incubated overnight at room temperature in a rabbit anti-synaptophysin IgG (1 : 500, Invitrogen) or a mouse anti-pan-axonal neurofilament IgG (1 : 500; SMI-312; Covance, Hornby, ON, Canada) primary antibody. Muscle fibers were then washed in PBS and incubated for 1 h in a goat anti-rabbit or goat anti-mouse IgG secondary antibody conjugated to Alexa Fluor 488 (1 : 500, Invitrogen). Fibers were finally washed in PBS and mounted in 50% glycerol/PBS mixture containing 0.03 mg/mL ρ-phenylenediamine.

The acetylcholine receptor (AChR) endplate morphology and NMJ innervation patterns are shown throughout as confocal projection images (*z*-stack collapsed confocal images) that were acquired using an LSM510 laser scanning confocal microscope (Zeiss Microimaging, Thornwood, NY, USA) and managed using LSM Image Browser (Zeiss Microimaging). Care was taken during acquisition of the confocal projection images that the laser scanned through the entire endplate and innervating axon.

The endplate areas, and degree of AChR fragmentation, were quantified from images digitally photographed using a wide-field fluorescence microscope equipped with a broad focal plane lens (Leica Microsystems, Bannockburn, IL, USA attached to a digital camera; C4742; Hamamatsu, Japan) (see also Rafuse *et al.*, 2000). Endplates were only used for quantification if the captured imaged accurately reflected the entire three-dimensional structure. Rhodamine-conjugated α-btx-binding areas were highlighted from background intensity using IPLAB software (Version 4.0; BD Biosciences). α-btx-binding areas were quantified by measuring the area occupied by the rhodamine fluorescence using IPLAB software. The number of discrete AChR fragments (a discrete fragment is defined as an uninterrupted, fluorescently α-btx-labeled AChR cluster within an individual NMJ region) (see also Hippenmeyer *et al.*, 2007) were quantified by individuals blinded to the experimental conditions.

Quantification of motoneuron and myofiber numbers

Spinal cords from cholera toxin subunit b-injected mice were sectioned longitudinally at 40 μm as previously described (Franz *et al.*, 2005). Raw cell counts were corrected by the Abercrombie method (Abercrombie, 1946). Whole muscle and individual muscle fiber cross-sectional areas were measured on slides stained for fast and slow myosin using IPLAB software (Version 4.0; BD Biosciences). The numbers of fast and slow fibers were enumerated by counting all of the fast and slow myosin-positive myofibers in a single section at the soleus midbelly. The sums of these counts closely agreed with an indirect assessment of the total number of fibers quantified by the ratio of whole muscle cross-sectional area: average muscle fiber cross-sectional area (30–60 fibers/muscle; 50% fast, 50% slow). Individuals blinded to the experimental conditions performed all of the quantifications.

Statistical analyses

A one-way ANOVA was performed to examine differences between groups over time. Tukey's honestly significant difference *post-hoc* test was used to determine where the significant differences occurred if the *F*-value exceeded F-critical. Two tailed-Student's *t*-tests were then used to make comparisons between genotypes at a given time-point. Statistical significance was considered to be achieved if $P < 0.05$.

Results

The stability of reinnervated neuromuscular junctions is compromised in mice lacking neural cell adhesion molecule

Synapse formation, function and stability were initially characterized by comparing the soleus muscle contractile force at 1, 3 and 6 months after crushing the tibial nerve 20 mm proximal to the soleus nerve/muscle entry point. At this distance, crushed sciatic motoneurons reinnervate all endplates in denervated shank muscles at 1 month after nerve injury (Magill *et al.*, 2007). For comparison, the same isometric tetanic contractions, elicited by a 50 Hz train of pulses (0.5 s train duration), were recorded from soleus muscles in unoperated wild-type and NCAM−/− mice (Fig. 1A). The isometric force profiles and rise times measured in this study are consistent with other studies

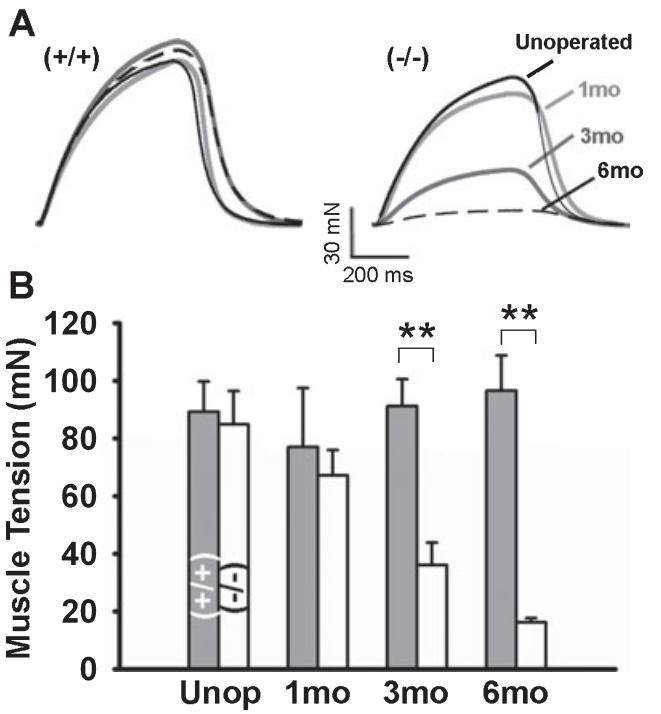

FIG. 1. Contractile force of reinnervated muscles in NCAM−/− mice decreases with time after injury. (A) Overlay of individual isometric tetanic force tracings shows that reinnervated wild-type (+/+) and NCAM−/− (light gray trace) soleus muscles generate the same amount of force as unoperated muscles (black trace) at 1 month after injury. In contrast to reinnervated wild-type muscles, NCAM−/− muscles did not maintain their force-generating capacity at 3 months after nerve crush injury (gray trace) and further declined 3 months later (black dashed trace). (B) Mean (+ SEM) tetanic muscle force generated by unoperated and reinnervated wild-type and NCAM−/− soleus muscles at 1, 3 and 6 months after tibial nerve crush injury. $^{**}P < 0.001$, two-tailed *t*-test. $n = 7$ muscles/group.

examining soleus muscle force production using similar *in-vitro* recording conditions (e.g. Witzemann *et al.*, 1996). As observed for medial gastrocnemius muscles (Rafuse *et al.*, 2000), unoperated soleus muscles in NCAM−/− mice generated the same amount of force as soleus muscles in wild-type mice (Fig. 1B). These results indicate that, under these stimulation parameters, the neurotransmission, excitation–contraction coupling and muscle fiber contractile properties are not noticeably compromised during development when NCAM is absent. The tetanic forces of reinnervated soleus muscles in wild-type and NCAM−/− mice were also not significantly different from each other at 1 month after nerve crush injury (Fig. 1A and B), indicating that motor axon regeneration and synapse reformation were not markedly affected in mice lacking NCAM (see also Moscoso *et al.*, 1998). Interestingly, however, reinnervated NCAM−/− soleus muscles did not maintain comparable force values as time passed. In fact, the tetanic force decreased significantly to about one-third of the wild-type values at 3 months after nerve injury (Fig. 1A and B; 3 months, wild-type vs. NCAM−/−, two-tailed *t*-test: $t_{12} = 4.81$, $P < 0.001$, $n = 7$ for each group) and further deteriorated at 6 months after injury (Fig. 1A and B; 6 months; $t_{12} = 7.63$, $P < 0.001$, $n = 7$ for each group).

Several factors can account for a loss of contractile strength over time. The force output would decrease if neurotransmission or excitation–contraction coupling was progressively compromised. The contractile force would also decline if reinnervated muscle fibers later atrophied or became denervated due to the withdrawal of axons. To address these possibilities we first analyzed EMGs recorded from unoperated and reinnervated wild-type and NCAM−/− soleus muscles during a train of stimuli (50 Hz, 0.5 s duration). Surface EMGs are the sum of all recorded motor unit action potentials. The peak-to-peak amplitude is proportional to the number and size of contracting muscle fibers (Henneman & Olson, 1965; Kosarov, 1974; Milner-Brown & Stein, 1975) in normal and reinnervated muscles (Totosy de Zepetnek *et al.*, 1991). A simultaneous decrease in force and EMG over time indicates that muscle fibers atrophied or degenerated (Kernell, 2006). A progressive decrease in force, in the absence of smaller EMGs, suggests that muscle fibers weakened due to metabolic or excitation–contraction coupling deficiencies.

The EMG peak-to-peak amplitudes did not differ between unoperated wild-type and NCAM−/− soleus muscles (Fig. 2C). Similarly, the amplitudes of the EMGs recorded from reinnervated soleus muscles in wild-type and NCAM−/− mice were not significantly different from each other at 1 month after nerve crush injury (Fig. 2C). However, as observed in the force recordings, EMGs from reinnervated NCAM−/− soleus muscles (Fig. 2B and C) were significantly smaller than those recorded from wild-type muscles at 3 months after nerve injury (Fig. 2A and C; 3 months, $t_{12} = 4.03$ $P < 0.001$, $n = 7$ for each group). The EMGs remained significantly smaller in NCAM−/− mice at 6 months after injury (data not shown). These results indicate that the loss of contractile force in NCAM−/− mice was due to muscle fiber atrophy and/or degeneration and not due to deficient excitation–contraction coupling or a progressive metabolic myopathy.

Reinnervated muscle fiber numbers decrease in mice lacking neural cell adhesion molecule

To determine whether the reinnervated soleus muscles in NCAM−/− mice contained smaller, or fewer, muscle fibers we quantified the whole muscle cross-sectional area, mean myofiber

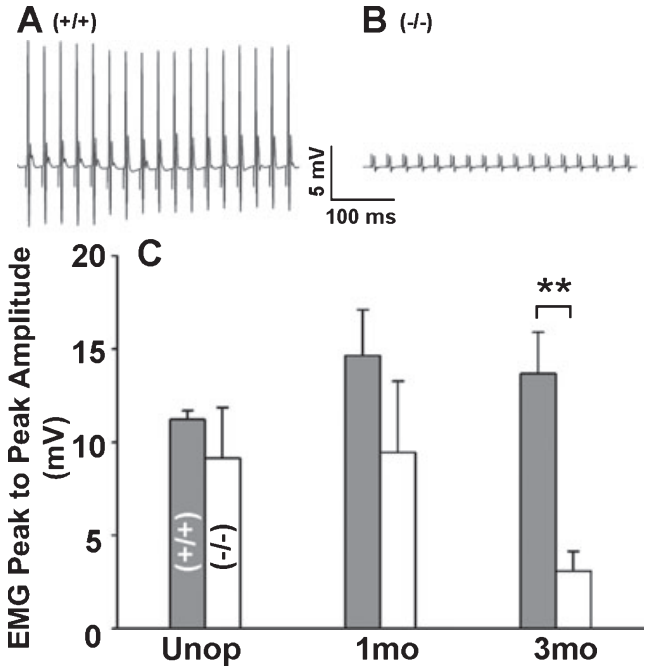

FIG. 2. EMGs recorded from reinnervated NCAM−/− soleus muscles are smaller than those recorded from wild-type muscles at 3 months after nerve injury. The amplitudes of EMGs recorded from a reinnervated NCAM−/− (B) soleus muscle were noticeably smaller than those recorded from reinnervated wild-type muscles (A) at 3 months after nerve injury (50 Hz stimulus train, 0.5 s duration). (C) Mean (+ SEM) EMG peak-to-peak amplitude recorded from unoperated and reinnervated wild-type (+/+) and NCAM−/− soleus muscles at 1 and 3 months after nerve injury. **$P < 0.001$, two-tailed *t*-test. $n = 7$ muscles/group.

cross-sectional area and the number of fast and slow myosin-expressing myofibers spanning the midbelly of unoperated and reinnervated muscles at 1, 3 and 6 months after nerve injury. Muscle cross-sections from wild-type and NCAM−/− mice were immunolabeled for fast (Fig. 3A and B) and slow (not shown) myosin heavy chains for better visualization. Gross morphological analysis (Fig. 3A and B) and cross-sectional area measurements (Fig. 3C) showed that soleus muscles in unoperated wild-type and NCAM−/− mice were the same size and had a similar fiber type distribution. As expected from the force recordings, reinnervated wild-type and NCAM−/− muscles were slightly smaller than unoperated muscles at 1 month after nerve injury (Fig. 3A–C; Unop.). The smaller muscle size was due to atrophy (Fig. 3D) rather than a loss of muscle fibers (Fig. 3E and F; 1 month). Muscle fiber atrophy is commonly observed in newly reinnervated muscles if they are denervated for at least 2 weeks (Magill *et al.*, 2007). As predicted from the force and EMG measurements, reinnervated NCAM−/− muscles began to deteriorate at 3 months after nerve injury (Fig. 3A and B; 3 months) and became significantly smaller than their wild-type counterpart after 6 months (Fig. 3C; 6 months; $t_8 = 3.17$, $P = 0.016$, $n = 5$ for each group). Interestingly, the decrease in muscle size was primarily due to the selective loss of fast muscle fibers, rather than continued myofiber atrophy (Fig. 3D), as indicated by the change in fast fiber morphology (Fig. 3A and B; 3 and 6 months) and number (Fig. 3E; 3 months; $t_8 = 6.2$, $P = 0.002$, 6 months; $t_8 = 4.93$, $P = 0.008$; $n = 5$ each group). On average, reinnervated soleus muscles in NCAM−/− mice contained only one-third of their normal complement of fast myosin-positive myofibers at 6 months after injury (Fig. 3E; 6 months). In contrast to fast myofibers, slow fiber

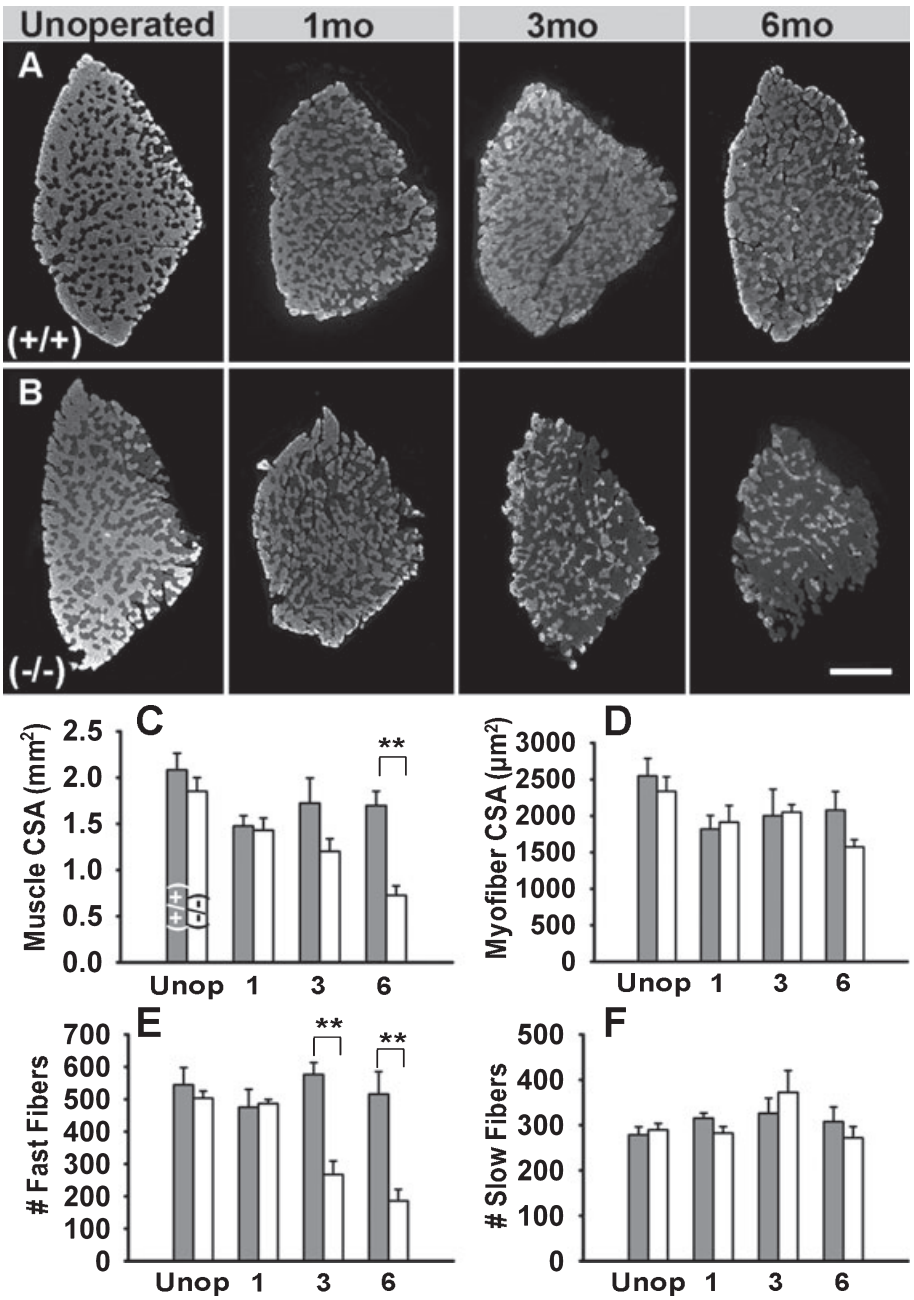

FIG. 3. Reinnervated soleus muscles in NCAM−/− mice decrease in size because they lose muscle fibers. Fast myosin-immunolabeled cross-sections from the midbelly of unoperated and reinnervated wild-type (A) and NCAM−/− (B) soleus muscles at 1, 3 and 6 months after nerve injury. Mean (+ SEM) muscle cross-sectional area (C), myofiber cross-sectional area (D), number of fast myosin-positive myofibers (E) and number of slow myosin-positive myofibers (F) in unoperated and reinnervated wild-type and NCAM−/− soleus muscles at 1, 3 and 6 months after nerve crush injury. $^{**}P < 0.02$; two-tailed *t*-test. $n = 5$ muscles/group. CSA, cross-sectional area. Scale bar: 500 μm.

numbers were unaffected by the absence of NCAM (Fig. 3F; 3 and 6 months).

Evidence for motor axon withdrawal in reinnervated NCAM−/− mice

Both denervation atrophy and muscular dystrophy (i.e. loss of muscle fibers without nervous system involvement) can result in muscle fiber degeneration. To assess which process was responsible for the loss of fibers in the reinnervated NCAM−/− mice we examined endplates for axon withdrawal using rhodamine-conjugated α-btx (to visualize AChRs) and neurofilament immunofluorescence. As expected, AChR-rich synaptic endplates in unoperated wild-type and NCAM−/− soleus muscles were innervated by a single motor axon that extended thin axonal neurofilament-positive branches into the junction (Fig. 4A and B). The same endplate morphology was observed in reinnervated wild-type mice at 3 months after injury (Fig. 4C). Although the majority of the reinnervated endplates in the NCAM−/− mice were normally innervated (data not shown), several endplates (12 of 90 from three different animals) showed signs of retracting or degenerating axons at 3 months after injury. For example, Fig. 4D shows a confocal projection image (i.e. collapsed z-stack containing all single optical images spanning through the endplate) of a thin axonal branch within the endplate (Fig. 4D; large arrow), which,

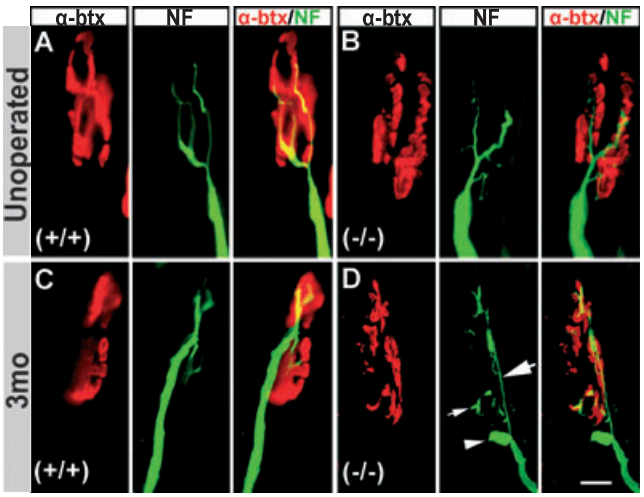

FIG. 4. Some reinnervated endplates in NCAM−/− mice at 3 months after injury show evidence of axon withdrawal. Rhodamine-conjugated α-btx-labeled AChRs in unoperated wild-type (A) and NCAM−/− (B) soleus muscles are innervated by a single motor axon extending into the NMJ via smaller neurofilament (NF)-immunopositive collaterals. (C) An NF-positive motor axon contacts rhodamine-conjugated α-btx-labeled AChRs at a reinnervated endplate in a wild-type soleus muscle at 3 months after nerve injury. NF staining is continuous along the axon shaft. (D) A representative confocal projection image showing signs of axonal withdrawal including a thin axonal branch (large arrow), which, in places, appears to disintegrate into a string of minute axonal remnants (small arrow). In addition, the proximal part of the axon resembles a retracting axonal bulb (arrowhead). Scale bar: 10 μm.

in places, appears to disintegrate into a string of minute remnants (Fig. 4D; small arrow). In addition, the proximal part of the axon resembles a retracting axonal bulb (Fig. 4D, arrowhead). This abnormal morphology is particularly notable because it is reminiscent of axonal bulb formation and axosome shedding exhibited by withdrawing axons during the elimination of polyneuronal innervation during post-natal development (Bishop *et al.*, 2004). Although not examined extensively, axonal withdrawal was not observed in reinnervated NCAM−/− soleus muscles at 1 month after injury ($n = 2$). Taken together, these observations support the notion that the loss of muscle fibers in reinnervated NCAM−/− soleus muscles was due in part to the withdrawal of motor axons.

Decreased muscle force and myofiber number are not due to motoneuron death

Muscle fiber denervation occurs if motoneurons die or if intact neurons withdraw some synapses. To distinguish between these two possibilities we quantified the number of motoneurons innervating unoperated and reinnervated soleus muscles in wild-type and NCAM−/− mice using standard cholera toxin subunit b backlabeling techniques. Consistent with previous studies (Franz *et al.*, 2005), unoperated wild-type and NCAM−/− mice contained the same number of soleus motoneurons (42.8 ± 2.86 and 45.70 ± 3.40; $n = 7$; $t_{13} = -0.662$, $P = 0.520$; $n = 8$ and 7 for wild-type and NCAM−/− mice, respectively). Interestingly, the numbers of motoneurons reinnervating soleus muscles in wild-type and NCAM−/− mice were not significantly different from each other at 3 months after nerve injury (38.27 ± 5.44 and 45.3 ± 3.72; $t_{11} = -1.10$, $P = 0.296$; $n = 6$ and 7 for wild-type and NCAM−/−, respectively) when force differences were clearly evident. These results indicate that the decrease in myofiber number was due to a reduction in motor unit size (i.e. the number of muscle fibers innervated by each motoneuron) rather than motoneuron death.

Neuromuscular transmitter release was compromised in reinnervated muscles in NCAM−/− mice

To determine whether the withdrawal of axons in the NCAM−/− mice correlated with defects in neuromuscular synaptic transmission, we performed intracellular recordings from individual soleus muscle fibers in unoperated and reinnervated wild-type and NCAM−/− mice. Low extracellular calcium was used to reduce the number of quanta released upon nerve stimulation to prevent action potentials in the muscle fibers (Everett & Ernst, 2004). Figure 5A and B shows typical mEPPs and seven evoked EPPs recorded from unoperated wild-type and NCAM−/− muscles. Under these conditions, none of the parameters measured were significantly different between unoperated wild-type and NCAM−/− mice, including: EPP amplitude, quantal content, percent failures (i.e. percentage of stimuli that failed to evoke an EPP), mEPP amplitude and mEPP frequency (Fig. 5F–J; $n = 5$ muscles/condition). Furthermore, all parameters measured were consistent with previous studies examining neurotransmission at mouse soleus NMJs under similar recording conditions (Jacob & Robbins, 1990; Everett & Ernst, 2004).

The amplitudes of the EPPs were significantly smaller (Fig. 5F), and the percentage of failures higher (Fig. 5H), in both experimental groups at 2 months after nerve injury. However, the quantal content (Fig. 5G) in both groups remained similar to unoperated values because there was a corresponding decrease in mean mEPP amplitude (Fig. 5I). Interestingly, two abnormal patterns of evoked responses emerged in NCAM−/− muscles (Fig. 5D and E, $n = 6$), but not wild-type muscles (Fig. 5C, $n = 5$), at 3 months after nerve injury. Some reinnervated NCAM−/− junctions exhibited an unusually large number of failed responses and had small EPPs (Fig. 5D). In another group of myofibers, the number of failures was normal but the distribution of EPPs was skewed to smaller values (Fig. 5E) compared with those recorded from wild-type fibers at the same time-point (Fig. 5C). As a consequence, the mean EPP amplitude (Fig. 5F; 3 months; $t_7 = 4.51$, $P < 0.001$; $n = 5$ for wild-type, $n = 4$ for NCAM−/−), quantal content (Fig. 5G; 3 months; $t_7 = 4.61$, $P < 0.001$; $n = 5$ for wild-type, $n = 4$ for NCAM−/−) and mEPP frequency (Fig. 5J; 3 months; $t_7 = 2.35$, $P = 0.0107$; $n = 5$ for wild-type, $n = 4$ for NCAM−/−) were all significantly less in NCAM−/− mice, compared with wild-type mice, at 3 months after nerve injury. In addition, the number of failures was higher at NCAM−/− NMJs compared with wild-type endplates at 3 months after injury (Fig. 5H; 3 months; $t_7 = -4.89$, $P < 0.001$; $n = 5$ for wild-type, $n = 4$ for NCAM−/−). Thus, the emergence of neurotransmission abnormalities correlated well with the appearance of withdrawing axons and the onset of muscle fiber degeneration. It is not known whether abnormal neurotransmission led to the withdrawal of axons (see Discussion).

Endplate morphology is abnormal in reinnervated NCAM−/− muscles

To determine whether a lack of NCAM leads to changes in NMJ morphology, we assayed AChR clusters at endplates using rhodamine-conjugated α-btx. The pre-synaptic morphology and alignment of synaptic structures were assessed using synaptophysin immunofluorescence. Figure 6 shows examples of projection confocal images of

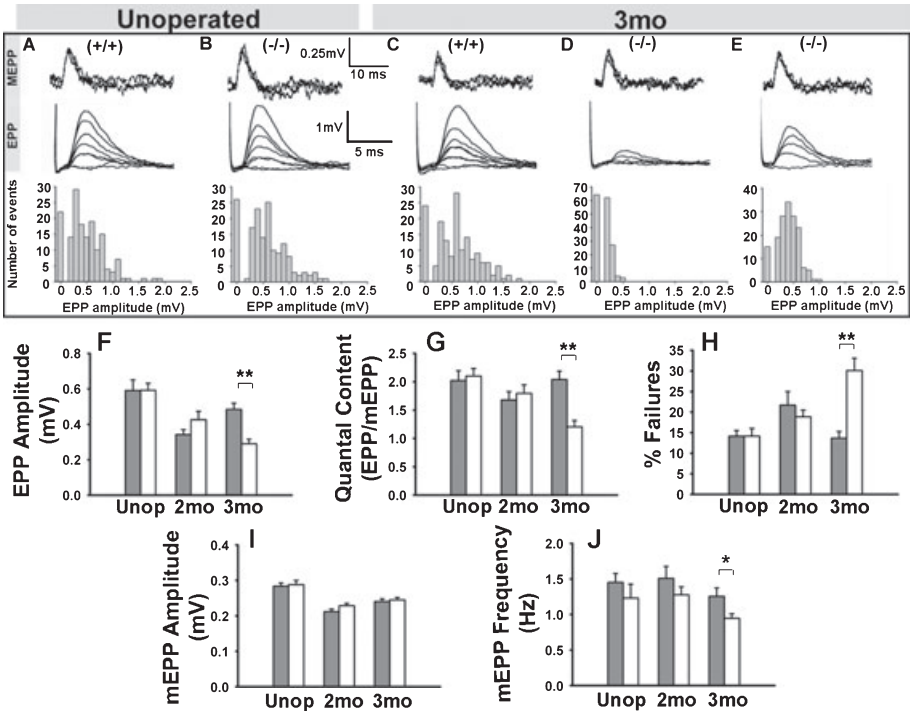

FIG. 5. Reinnervated NCAM−/− mice begin to exhibit alterations in transmitter release properties at 3 months after nerve injury. Representative mEPPS and EPPs recorded from unoperated soleus muscles in wild-type (A) and NCAM−/− (B) mice. Representative mEPPs and EPPs recorded from reinnervated wild-type (C) and NCAM−/− (D and E) muscles at 3 months after injury. Some reinnervated NCAM−/− junctions exhibited a large number of failed responses and only elicited small EPPs (D), whereas others had evoked EPPs that were skewed to smaller values (E). Frequency histograms are for all EPPs recorded from the myofiber shown above. Failures are scored at 0 mV. Mean (+ SEM) EPP amplitude (F), quantal content (G), % failures (H), mEPP amplitude (I) and mEPP frequency (J). $^{**}P < 0.001$, $^{*}P < 0.02$, two-tailed *t*-tests. $n = 5$ wild-type muscles; $n = 6$ NCAM−/− muscles.

α-btx-positive AChR clusters and the pre-synaptic morphology in endplates from unoperated wild-type and NCAM−/− mice (Fig. 6A and B). As observed in unoperated diaphragm and semitendinosus muscles in NCAM−/− mice (Moscoso *et al.*, 1998; Rafuse *et al.*, 2000), the vast majority of the pre-synaptic and post-synaptic components were normally aligned and showed no gross abnormalities. However, because endplates are complex structures including regions of high AChR density interspersed with regions lacking AChRs, we decided to quantify endplate size in two ways: (i) the total rhodamine-conjugated α-btx-binding area and (ii) the number of uninterrupted, discrete fragments (see Materials and methods). As expected, AChRs were distributed in one to two uninterrupted fragments per NMJ (Fig. 6A and F) in wild-type mice and α-btx binding occupied a surface area of ∼300 μm^2 (Fig. 6E). Compared with wild-type mice, AChRs in unoperated NCAM−/− mice were distributed in more fragments per NMJ (Fig. 6F; $t_7 = -5.62$, $P < 0.001$; $n = 5$ for wild-type, $n = 4$ for NCAM−/−). However, despite the larger number of isolated clusters, α-btx-positive AChRs occupied a significantly smaller area (Fig. 6E; $t_7 = 3.10$, $P = 0.00131$; $n = 5$ for wild-type, $n = 4$ for NCAM−/−) (see also Moscoso *et al.*, 1998; Rafuse *et al.*, 2000).

The α-btx-positive area (Fig. 6C and E) and number of AChR fragments (Fig. 6C and F) gradually increased over time in reinnervated wild-type muscles. Examination of contralateral muscles at later time-points revealed that this increase in endplate fragmentation is directly related to reinnervation and is not a consequence of the aging process (data not shown). Interestingly, the α-btx-binding area (Fig. 6E) and number of discrete fragments (Fig. 6F) were essentially the same between the three different groups (i.e. unoperated, 2 and 3 months after nerve injury) in the NCAM−/− mice (Fig. 6E and F). Consequently, although endplates in NCAM−/− mice are different from wild-type, progressive changes in their morphology do not appear to precipitate the observed decrease in muscle function at 3 months after nerve injury.

Lack of neural cell adhesion molecule in motoneurons or muscle fibers alone does not lead to synaptic dysfunction

The NMJ is a tripartite synapse consisting of a pre-synaptic motoneuron, post-synaptic muscle fiber and peri-synaptic tSC. Each cell type expresses NCAM at the adult NMJ (Rieger *et al.*, 1985; Covault & Sanes, 1986). As a result, the disorders observed in reinnervated NCAM−/− mice could be due to a loss of NCAM pre-synaptically, post-synaptically and/or peri-synaptically. To help distinguish between these possibilities, we generated mutant mice in which the floxed NCAM gene (Bukalo *et al.*, 2004) was inactivated by cre-recombinase under the control of the Hb9 (Yang *et al.*, 2001) or HSA (Miniou *et al.*, 1999; Cifuentes-Diaz *et al.*, 2001) promoter. This breeding strategy selectively abolishes NCAM expression in motoneurons (mice termed $NCAM^{flx/flx}/Hb9^{cre/+}$; see Franz *et al.*, 2008) and NCAM expression in muscle fibers (mice termed $NCAM^{flx/flx}/HSA^{cre/+}$; see Supporting information, Fig. S1), respectively. The selective excision of NCAM from tSCs was not performed due to the absence of genes specifically expressed by tSCs. Surprisingly, neither the $NCAM^{flx/flx}/Hb9^{cre/+}$ or $NCAM^{flx/flx}/HSA^{cre/+}$ mutants exhibited deficits in whole muscle tension (Fig. 7A) or evoked neurotransmission (i.e. mean EPP amplitude, mean quantal content and mean % failures; Fig. 7B) before, or at 3 months after, nerve injury. The mutant mice, however, had some irregularities. Functionally, mEPPs were significantly larger

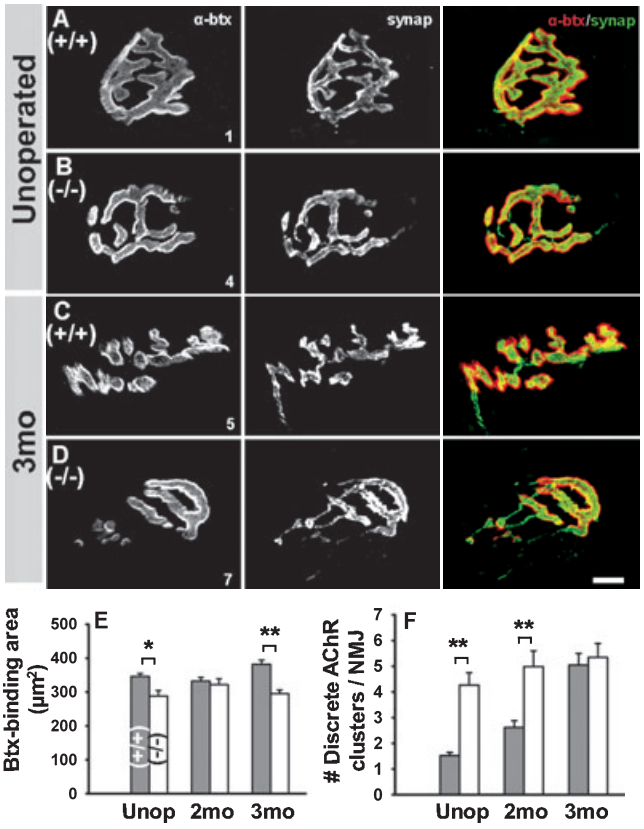

FIG. 6. Morphology of endplates in unoperated and reinnervated wild-type and NCAM−/− soleus muscles. (A–D) α-btx-positive AChRs in unoperated wild-type (A) and NCAM−/− (B) mice aligned with pre-synaptic structures as revealed by antibodies to synaptophysin. However, the number of uninterrupted, discrete fragments of α-btx-positive AChRs was higher in unoperated NCAM−/− junctions (B) compared with wild-type (A). Pre-synaptic and post-synaptic structures are also similarly aligned in reinnervated wild-type (C) and NCAM−/− (D) soleus muscles at 3 months after injury. Interestingly, the number of uninterrupted, discrete fragments of α-btx-positive AChRs at wild-type endplates (C) increased to levels similar to reinnervated NCAM−/− junctions (D). Mean (+ SEM) α-btx-binding area/NMJ (E) and number of discrete AChR clusters/NMJ (F) (n = 72–124 endplates). *P = 0.00131, **$P < 0.001$, two-tailed t-test. n = 5 wild-type muscles; n = 4 NCAM−/− muscles. Scale bar: 10 μm.

than normal in both conditional mutants at 3 months after injury (Fig. 7B; 3 months; wild-type vs. $NCAM^{flx/flx}/Hb9^{cre/+}$; $t_8 = -4.60$, $P < 0.001$; $n = 5$ for both; wild-type vs. $NCAM^{flx/flx}/HSA^{cre/+}$; $t_8 = -5.02$, $P < 0.001$; $n = 5$ for both), whereas the frequency of mEPPs at reinnervated NMJs in $NCAM^{flx/flx}/Hb9^{cre/+}$ was less than that observed in wild-type mice (data not shown).

Interestingly, NMJs were significantly larger than normal in unoperated $NCAM^{flx/flx}/Hb9^{cre/+}$ and $NCAM^{flx/flx}/HSA^{cre/+}$ mice (Fig. 7C; Unop. wild-type vs. $NCAM^{flx/flx}/Hb9^{cre/+}$; $t_8 = -3.19$, $P < 0.001$, $n = 5$ for both; Unop. wild-type vs. $NCAM^{flx/flx}/HSA^{cre/+}$; $t_8 = -4.07$, $P < 0.001$, $n = 5$ for both). The discrepancy between reduced growth at NCAM−/− junctions and increased growth at conditional mutant junctions may partially be explained by observations in *Drosophila*, where a 50% reduction in the expression of the NCAM homolog Fasciclin II at the NMJ results in enhanced synaptic growth, whereas a complete knockout of Fasciclin II resulted in reduced synaptic growth, destabilization and eventual withdrawal (Schuster *et al.*, 1996; Landmesser, 1997). In addition, both conditional mutants contained significantly more AChR fragments than unoperated wild-type mice (Fig. 7C; Unop. wild-type vs. $NCAM^{flx/flx}/Hb9^{cre/+}$, $t_8 = -4.90$, $P < 0.001$, $n = 5$ for both; Unop. wild-type vs. $NCAM^{flx/flx}/HSA^{cre/+}$, $t_8 = -5.39$, $P < 0.001$, $n = 5$ for both), with endplates in $NCAM^{flx/flx}/HSA^{cre/+}$ mice being the most fragmented (Fig. 7C; Unop. $NCAM^{flx/flx}/Hb9^{cre/+}$ vs. $NCAM^{flx/flx}/HSA^{cre/+}$, $t_8 = -2.07$, $P = 0.0203$, $n = 5$ for both). Interestingly, endplates in unoperated $NCAM^{flx/flx}/HSA^{cre/+}$ mice contained the same number of AChR fragments as those in NCAM−/− mice (Fig. 6F). These results suggest that muscle-derived and, to a lesser extent, neural-derived NCAM plays a role in establishing a normal distribution of AChRs during development. Endplates in all three experimental groups were more fragmented than their unoperated counterparts at 3 months after injury (Fig. 7C). Taken together, whereas pre-synaptic and post-synaptic NCAM is important for normal endplate development, the loss of either one alone is not sufficient to recapitulate the functional deficits observed in reinnervated NCAM−/− mice.

Discussion

Although NCAM is not essential for motor axon regeneration or synaptic formation during development (Moscoso *et al.*, 1998; Franz *et al.*, 2005), our results indicate that it is required for maintaining normal muscle function after a peripheral nerve injury. The most striking neuromuscular irregularities detected at 3 months after nerve injury include a significant decrease in contractile force, loss of fast muscle fibers, signs of inappropriate axonal withdrawal and impaired synaptic neurotransmission. Interestingly, selective ablation of NCAM from motoneurons, or muscle fibers, did not mimic the deficiencies observed in the NCAM−/− mice, suggesting that NCAM must be absent pre-synaptically and post-synaptically or absent on peri-synaptic tSCs in order to destabilize the synapse after reinnervation.

Although NCAM−/− mice show signs of increased neuromuscular fatigue (Polo-Parada *et al.*, 2001), nerve/muscle development and function are not dramatically compromised. In the light of the current results, it seems reasonable to assume that additional adhesion/signaling molecules compensate for the lack of NCAM during embryonic development. Although the process of peripheral nerve regeneration is often described as a recapitulation of developmental processes, this description is inappropriate because many genes expressed during embryogenesis are not re-expressed during regeneration (Bosse *et al.*, 2006). This raises the possibility that molecules compensating for the lack of NCAM during development are not re-expressed after nerve injury. Consequently, the phenotypes described in the present study may reflect the true function of NCAM at the NMJ when compensation is less complete and may not be limited to its function after injury.

Neural cell adhesion molecule, neurotransmission, synaptic stabilization and sprouting

Three unusual, and potentially related, events occurred in NCAM−/− mice at 3 months after injury. First, neurotransmission became compromised at a subset of NMJs. Second, there was a selective loss of fast myofibers. Third, the decrease in fast myofibers was not accompanied by a simultaneous increase in slow muscle fibers (see below). Because fast and slow motoneurons innervate fast and slow muscle fibers, respectively (Kernell, 2006), these results suggest that fast motoneurons withdrew axons, whereas slow motoneurons did not. Motor axon withdrawal is a natural phenomenon occurring during the elimination of polyneuronal innervation in developing muscles

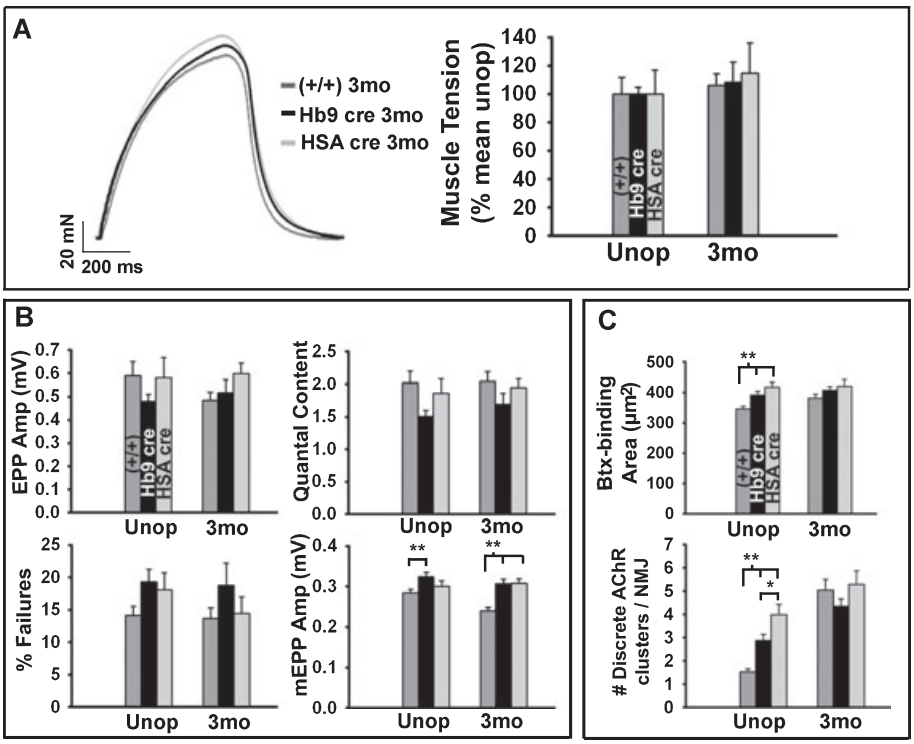

FIG. 7. Conditional ablation of NCAM from motoneurons or muscle fibers does not disrupt neuromuscular function at 3 months after nerve injury. (A) Overlay of individual isometric tetanic force tracings and quantification (% mean unoperated + SEM) indicated that reinnervated wild-type, $NCAM^{flx/flx}/Hb9^{cre/+}$ and $NCAM^{flx/flx}/HSA^{cre/+}$ soleus muscles generated the same amount of force as unoperated muscles at 3 months after injury. (B) NMJs in reinnervated $NCAM^{flx/flx}/Hb9^{cre/+}$ and $NCAM^{flx/flx}/HSA^{cre/+}$ mice had normal evoked neurotransmitter release properties (mean EPP amplitude, mean quantal content and % failures). However, the amplitudes of mEPPs were significantly larger than normal in both transgenic mice at 3 months after injury. (C) Morphology of AChR clusters is abnormal in unoperated $NCAM^{flx/flx}/Hb9^{cre/+}$ and $NCAM^{flx/flx}/HSA^{cre}$ soleus muscles. Interestingly, morphological differences between endplates in the three strains of mice dissipated after injury (n = 6 muscles/group for whole muscle physiology; n = 38–55 fibers from five muscles/group for intracellular recordings; n = 58–83 endplates from five muscles/group for endplate morphology). *P = 0.0203, **P < 0.001, two-tailed t-test. n = 5 muscles/group.

(Redfern, 1970; Brown *et al.*, 1976). Although the precise mechanisms underlying this phenomenon are not understood, it is well established that the quantal content of the remaining axons becomes increasingly greater than those destined to withdraw (Colman *et al.*, 1997; Kopp *et al.*, 2000). This disparity ultimately contributes to the withdrawal of the weaker synapse (Colman *et al.*, 1997). In the present study, the quantal content became significantly less in reinnervated NCAM−/− mice when a loss of fast muscle fibers was first detected and when fast motor axons were presumably withdrawing. Based on the developmental studies, it is tempting to speculate that the synaptic instability of fast motoneurons in reinnervated NCAM−/− mice was, in part, because their quantal content was insufficient to signal continued maintenance of the terminal.

The withdrawal of motor axons from a subset of muscle fibers results in a state of partial denervation. Normally, motoneurons have a tremendous capacity to sprout and functionally innervate up to five times as many muscle fibers as normal in partially denervated (Thompson & Jansen, 1977; Brown & Ironton, 1978; Gorio *et al.*, 1983; Fisher *et al.*, 1989; Yang *et al.*, 1990; Rafuse *et al.*, 1992; Gordon *et al.*, 1993) and reinnervated (Rafuse & Gordon, 1996) muscles. When slow motoneurons sprout and innervate denervated fast fibers they convert their biochemical and contractile properties to become those of slow fibers (Kernell, 2006). Taken together, these results suggest that slow motoneurons did not sprout and functionally innervate fast fibers that became denervated at 3-6 months after injury in the NCAM−/− mice. The quantal content is less at reinnervated NCAM−/− junctions (Fig. 5) and at sprouted terminals in partially denervated mouse muscles (Rochel & Robbins, 1988). Consequently, the lack of slow motoneuron sprouting may be due to their inability to release enough neurotransmitter at the sprouted terminals to sufficiently stabilize the synapse. Alternatively, the lack of NCAM on tSCs may impede the growth of sprouts to denervated endplates (see below).

It is not known why the quantal content became less at reinnervated endplates in NCAM−/− mice at 3 months after injury. The normality of neurotransmission in mice with NCAM-deficient motoneurons, or muscle fibers (Fig. 5), suggests that NCAM must be absent both presynaptically and post-synaptically or absent from tSCs to alter neurotransmission after a nerve injury. The latter possibility is worth noting because neurotransmitters released during high-frequency stimulation, as occurs when fast motoneurons are depolarized (Grimby *et al.*, 1979), activate G-protein-coupled receptors on tSCs and cause the release of intracellular Ca^{2+} from internal stores (Robitaille, 1998). These tSC Ca^{2+} transients can in turn potentiate neurotransmitter release at the NMJ (Castonguay & Robitaille, 2001; Colomar & Robitaille, 2004). This notion is supported by studies in adult frogs where the selective ablation of tSCs leads to a decrease in quantal content, axon withdrawal and decline in contractile force 1 week later (Reddy *et al.*, 2003). Like the present study, these deficits were not accompanied by changes in the amplitude of mEPPs (Reddy *et al.*, 2003; Feng & Ko, 2008). Finally, at least one study has identified a lack of tSCs localized to frog NMJs following reinnervation in the presence of functional blocking antibodies to NCAM (Rieger *et al.*, 1988).

Pre-synaptic neural cell adhesion molecule signaling

Neural cell adhesion molecule interacts with a number of axonal intracellular molecules that are important for synapse stabilization. For example, spectrin copurifies with the 180 kD isoform of NCAM in adult mouse brain protein fractions (Pollerberg *et al.*, 1987). NCAM-180 is selectively targeted from the axonal shaft to the pre-synaptic terminals of motoneurons after myotube contact *in vitro* (Hata *et al.*, 2007). In cultured hippocampal neurons, contacts between axons and dendrites transform into functional synapses, in part, because synaptic proteins within the trans-Golgi network organelles are linked to clusters of NCAM in the plasma membrane via spectrin (Sytnyk *et al.*, 2004). Heterotetramers of α-spectrin and ß-spectrin subunits also form spectrin–actin filamentous scaffoldings that are important in maintaining plasma membrane integrity and cytoskeletal structure (Bennett & Baines, 2001). The selective loss of pre-synaptic spectrin at mature NMJs in *Drosophila* leads to a decrease in quantal content and synapse elimination (Featherstone *et al.*, 2001; Pielage *et al.*, 2005). Interestingly, Fasciclin II is removed at sites of retraction prior to synapse withdrawal when pre-synaptic spectrin is experimentally reduced (Pielage *et al.*, 2005). Taken together, it is tempting to speculate that spectrin helps to stabilize newly formed NMJs through its interaction with NCAM. However, unlike *Drosophila* (Schuster *et al.*, 1996), our results from $NCAM^{flx/flx}/Hb9^{cre/+}$ mice indicate that the loss of pre-synaptic NCAM alone is not sufficient to precipitate neurotransmission dysfunction or axon withdrawal in mice.

Post-synaptic neural cell adhesion molecule signaling

Neural cell adhesion molecule initiates signaling by activating intracellular signaling molecules such as Fyn (reviewed by Maness & Schachner, 2007; Ditlevsen *et al.*, 2008). Fyn and Src, members of the Src family of non-receptor tyrosine kinases, functionally interact with AChRs in myofibers *in vitro* (Fuhrer & Hall, 1996) and *in vivo* (Smith *et al.*, 2001). Interestingly, muscle development, motor axon pathfinding and AChR clustering are normal in Fyn/Src double mutant mice (Smith *et al.*, 2001), indicating that they are not essential for neuromuscular development. However, disruption of their function post-natally results in AChR fragmentation (Sadasivam *et al.*, 2005) in a manner that is very similar to that observed in NCAM−/− and $NCAM^{flx/flx}/HSA^{cre/+}$ mice (Figs 6 and 7). It is therefore possible that increased fragmentation of AChRs in NCAM−/− muscle fibers is due to a lack of NCAM-mediated Fyn/Src signaling.

Peri-synaptic neural cell adhesion molecule signaling

Non-injured motoneurons in partially denervated muscles grow axonal sprouts along tSC bridges that form between innervated and denervated endplates (Son & Thompson, 1995). This expansion in motor unit size can functionally compensate for an 80% loss in motoneuron number before a decline in contractile force is observed in partially denervated muscles (e.g. Brown & Ironton, 1978; Rafuse *et al.*, 1992). Thus, it was somewhat surprising to find that slow motoneurons did not sprout collaterals to functionally innervate denervated fast myofibers. The absence of axonal sprouting could be explained if tSC bridges did not form or they were less conducive for growth. Several growth pathways are stimulated through NCAM activation. For example, NCAM-mediated growth requires the activation of fibroblast growth factor receptor and recruitment of protein kinase C β_2 to detergent-insoluble lipid rafts (Neithammer *et al.*, 2002; Leshchyns'ka *et al.*, 2003). This fibroblast growth factor receptor/protein kinase C pathway can then associate with growth-associated molecules such as growth associated protein 43 (GAP-43), cortical cytoskeleton-associated protein 23 (CAP-23) and myristoylated alanine-rich C kinase substrate (MARCKS) (Laux *et al.*, 2000). GAP-43 has been implicated in NCAM-mediated neurite outgrowth (Meiri *et al.*, 1998; Korshunova *et al.*, 2007) and is significantly up-regulated by tSCs after injury (Woolf *et al.*, 1992). Consequently, NCAM-mediated growth mechanisms may participate in the extension of sprouts along tSC bridges in partially denervated muscles (Reynolds & Woolf, 1992; Son & Thompson, 1995).

Neural cell adhesion molecule and neuromuscular disorders

Although motor unit dysfunction is often thought to result from motoneuron death in motoneuron disease, it is not known whether this reflects the actual sequence of pathological events (Rich *et al.*, 2002). For example, abnormalities in synaptic function (including decreased quantal content) occur while motoneurons are still capable of producing action potentials in patients with ALS (Maselli *et al.*, 1993). Mice expressing mutant superoxide dismutase 1 (SOD1) die due to muscle denervation even when motoneuron death is prevented (Gould *et al.*, 2006). The decreased release of transmitter from motor terminals underlies motor unit dysfunction, and probably death, in hereditary canine spinal muscular atrophy (Rich *et al.*, 2002). Interestingly, like the preferential withdrawal of fast motoneurons in the present study, the largest motoneurons are usually the first to succumb to motoneuron disease (Kernell, 2006). In addition, polysialylated NCAM is induced in surviving motoneurons in SOD1 mutant mice (Warita *et al.*, 2001). Although NCAM is routinely used to identify denervated fibers in animal models of ALS (e.g. Hegedus *et al.*, 2008), recent studies have challenged the notion that NCAM is up-regulated on myofibers only after denervation (Grumbles *et al.*, 2008). Consequently, motoneurons and muscle fibers may actually up-regulate NCAM in response to disease-related challenges, in an attempt to stabilize the synapse. Whether NCAM dysfunction contributes to motoneuron disease is not known but results from the present study suggest that this notion is worth pursuing.

Supporting Information

Additional supporting information may be found in the online version of this article:

Fig. S1. NCAM immunostaining is absent from 4 day denervated NCAM−/− and $NCAM^{flx/flx}/HSA^{cre/+}$ but elevated in wild-type and $NCAM^{flx/flx}/Hb9^{cre/+}$ soleus muscles.

Please note: As a service to our authors and readers, this journal provides supporting information supplied by the authors. Such materials are peer-reviewed and may be re-organized for online delivery, but are not copy-edited or typeset by Wiley-Blackwell. Technical support issues arising from supporting information (other than missing files) should be addressed to the authors.

Acknowledgements

This work was supported by a grant from the Canadian Institutes for Health Research (V.F.R.). C.K.F. and P.H.C. were funded by graduate student scholarship awards from the Natural Sciences and Engineering Research Council of Canada. We would like to acknowledge the excellent technical assistance of Lindsay Fisher, Crystal Milligan, Kathleen Connolly and Simone Laforest. The S58 antibody was obtained from the Developmental Studies Hybridoma Bank under the auspices of the National Institute of Child Health and Human Development and maintained by the University of Iowa Department of Biology. Finally, we would like to thank Dr Lynn Landmesser for her helpful comments during the preparation of this manuscript.

Abbreviations

AChR, acetylcholine receptor; ALS, amyotrophic lateral sclerosis; α-btx, α-bungarotoxin; EMG, electromyogram; EPP, endplate potential; Hb9, human homeobox gene 9; HSA, human α-skeletal actin; mEPP, miniature endplate potential; NCAM, neural cell adhesion molecule; NMJ, neuromuscular junction; PBS, phosphate-buffered saline; tSC, terminal Schwann cell.

References

Abercrombie, M. (1946) Estimation of nuclear population from microtome sections. *Anat. Neurobiol. Rec.*, **94**, 239–247.

Bennett, V. & Baines, A.J. (2001) Spectrin and ankyrin-based pathways: metazoan inventions for integrating cells into tissues. *Physiol. Rev.*, **81**, 1353–1392.

Bishop, D.L., Misgeld, T., Walsh, M.K., Gan, W.B. & Lichtman, J.W. (2004) Axon branch removal at developing synapses by axosome shedding. *Neuron*, **44**, 651–661.

Bosse, F., Hasenpusch-Theil, K., Küry, P. & Müller, H.W. (2006) Gene expression profiling reveals that peripheral nerve regeneration is a consequence of both novel injury-dependent and reactivated developmental processes. *J. Neurochem.*, **96**, 1441–1457.

Brown, M.C. & Ironton, R. (1978) Sprouting and regression of neuromuscular synapses in partially denervated mammalian muscles. *J. Physiol.*, **278**, 325–348.

Brown, M.C., Jansen, J.K. & Van Essen, D. (1976) Polyneuronal innervation of skeletal muscle in new-born rats and its elimination during maturation. *J. Physiol.*, **261**, 387–422.

Bukalo, O., Fentrop, N., Lee, A.Y., Salmen, B., Law, J.W., Wotjak, C.T., Schweizer, M., Dityatev, A. & Schachner, M. (2004) Conditional ablation of the neural cell adhesion molecule reduces precision of spatial learning, long-term potentiation, and depression in the CA1 subfield of mouse hippocampus. *J. Neurosci.*, **24**, 1565–1577.

Castonguay, A. & Robitaille, R. (2001) Differential regulation of transmitter release by presynaptic and glial Ca^{2+} internal stores at the neuromuscular synapse. *J. Neurosci.*, **21**, 1911–1922.

Cifuentes-Diaz, C., Frugier, T., Tiziano, F.D., Lacène, E., Roblot, N., Joshi, V., Moreau, M.H. & Melki, J. (2001) Deletion of murine SMN exon 7 directed to skeletal muscle leads to severe muscular dystrophy. *J. Cell Biol.*, **152**, 1107–1114.

Colman, H., Nabekura, J. & Lichtman, J.W. (1997) Alterations in synaptic strength preceding axon withdrawal. *Science*, **275**, 356–361.

Colomar, A. & Robitaille, R. (2004) Glial modulation of synaptic transmission at the neuromuscular junction. *Glia*, **47**, 284–289.

Conforti, L., Adalbert, R. & Coleman, M.P. (2007) Neuronal death: where does the end begin? *Trends Neurosci.*, **30**, 159–166.

Covault, J. & Sanes, J.R. (1986) Distribution of N-CAM in synaptic and extrasynaptic portions of developing and adult skeletal muscle. *J. Cell Biol.*, **102**, 716–730.

Cremer, H., Lange, R., Christoph, A., Plomann, M., Vopper, G., Roes, J., Brown, R., Baldwin, S., Kraemer, P., Scheff, S., Barthels, D., Rajewski, K. & Wille, W. (1994) Inactivation of the N-CAM gene in mice results in size reduction of the olfactory bulb and deficits in spatial learning. *Nature*, **367**, 455–459.

Ditlevsen, D.K., Povlsen, G.K., Berezin, V. & Bock, E. (2008) NCAM-induced intracellular signaling revisited. *J. Neurosci. Res.*, **86**, 727–743.

Everett, A.W. & Ernst, E.J. (2004) Increased quantal size in transmission at slow but not fast neuromuscular synapses of apolipoprotein E deficient mice. *Exp. Neurol.*, **185**, 290–296.

Featherstone, D.E., Davis, W.S., Dubreuil, R.R. & Broadie, K. (2001) Drosophila α- and *β*-spectrin mutations disrupt presynaptic neurotransmitter release. *J. Neurosci.*, **21**, 4215–4224.

Feng, Z. & Ko, C.P. (2008) Schwann cells promote synaptogenesis at the neuromuscular junction via transforming growth factor-beta1. *J. Neurosci.*, **28**, 9599–9609.

Fisher, T.J., Vrbová, G. & Wijetunge, A. (1989) Partial denervation of the rat soleus muscle at two different developmental stages. *Neuroscience*, **28**, 755–763.

Franz, C.K., Rutishauser, U. & Rafuse, V.F. (2005) Polysialylated neural cell adhesion molecule is necessary for selective targeting of regenerating motor neurons. *J. Neurosci.*, **25**, 2081–2091.

Franz, C.K., Rutishauser, U. & Rafuse, V.F. (2008) Intrinsic neuronal properties control selective targeting of regenerating motoneurons. *Brain*, **131**, 1492–1505.

Frey, D., Schneider, C., Xu, L., Borg, J., Spooren, W. & Caroni, P. (2000) Early and selective loss of neuromuscular synapse subtypes with low sprouting competence in motoneuron diseases. *J. Neurosci.*, **20**, 2534–2542.

Fuhrer, C. & Hall, Z.W. (1996) Functional interaction of Src family kinases with the acetylcholine receptor in C2 myotubes. *J. Biol. Chem.*, **271**, 32474–32481.

Gordon, T., Yang, J.F., Ayer, K., Stein, R.B. & Tyreman, N. (1993) Recovery potential of muscle after partial denervation: a comparison between rats and humans. *Brain Res. Bull.*, **30**, 477–482.

Gorio, A., Carmignoto, G., Finesso, M., Polato, P. & Nunzi, M.G. (1983) Muscle reinnervation – II. Sprouting, synapse formation and repression. *Neuroscience*, **8**, 403–416.

Gould, T.W., Buss, R.R., Vinsant, S., Prevette, D., Sun, W., Knudson, C.M., Milligan, C.E. & Oppenheim, R.W. (2006) Complete dissociation of motor neuron death from motor dysfunction by Bax deletion in a mouse model of ALS. *J. Neurosci.*, **26**, 8774–8786.

Grimby, L., Hannerz, J. & Hedman, B. (1979) Contraction time and voluntary discharge properties of individual short toe extensor motor units in man. *J. Physiol.*, **289**, 191–201.

Grumbles, R.M., Almeida, V.W. & Thomas, C.K. (2008) Embryonic neurons transplanted into the tibial nerve reinnervate muscle and reduce atrophy but NCAM expression persists. *Neurol. Res.*, **30**, 183–189.

Gu, Z., Steinmetz, L.M., Gu, X., Scharfe, C., Davis, R.W. & Li, W.H. (2003) Role of duplicate genes in genetic robustness against null mutations. *Nature*, **421**, 63–66.

Harrelson, A.L. & Goodman, C.S. (1988) Growth cone guidance in insects: fasciclin II is a member of the immunoglobulin superfamily. *Science*, **242**, 700–708.

Hata, K., Polo-Parada, L. & Landmesser, L.T. (2007) Selective targeting of different neural cell adhesion molecule isoforms during motoneuron-myotube synapse formations in culture and the switch from an immature to mature form of vesicle cycling. *J. Neurosci.*, **27**, 14481–14493.

Hegedus, J., Putman, C.T., Tyreman, N. & Gordon, T. (2008) Preferential motor unit loss in the SOD1 G93A transgenic mouse model of amyotrophic lateral sclerosis. *J. Physiol.*, **586**, 3337–3351.

Henneman, E. & Olson, C.B. (1965) Relations between structure and function in the design of skeletal muscles. *J. Neurophysiol.*, **28**, 581–598.

Hippenmeyer, S., Huber, R.M., Ladle, D.R., Murphy, K. & Arber, S. (2007) ETS transcription factor Erm controls subsynaptic gene expression in skeletal muscles. *Neuron*, **55**, 726–740.

Jacob, J.M. & Robbins, N. (1990) Differential effects of age of neuromuscular transmission in partially denervated mouse muscle. *J. Neurosci.*, **10**, 1522–1529.

Kernell, D. (2006) *The Motoneurone and its Muscle Fibres*. Oxford University Press, New York.

Kong, L., Wang, X., Choe, D.W., Polley, M., Burnett, B.G., Bosch-Marcé, M., Griffin, J.W., Rich, M.M. & Sumner, C.J. (2009) Impaired synaptic vesicle release and immaturity of neuromuscular junctions in spinal muscular atrophy mice. *J. Neurosci.*, **29**, 842–851.

Kopp, D.M., Perkel, D.J. & Balice-Gordon, R.J. (2000) Disparity in neurotransmitter release probability among competing inputs during neuromuscular synapse elimination. *J. Neurosci.*, **20**, 8771–8779.

Korshunova, I., Noviskaya, V., Kirushko, D., Pedersen, N., Kolkova, K., Kropotova, E., Mosevitsky, M., Rayko, M., Morrow, J.S., Ginzburg, I., Berezin, V. & Bock, E. (2007) GAP-43 regulates NCAM-180-mediated neurite outgrowth. *J. Neurochem.*, **100**, 1599–1612.

Kosarov, D. (1974) Vectorelectromyographic control on the position of surface electrodes in relation to active motor units in the human muscles. *Acta Physiol. Pharmacol. Bulg.*, **1**, 85–93.

Landmesser, L. (1997) Synaptic plasticity: fastening synapses by adhesion. *Curr. Biol.*, **7**, R28–R30.

Laux, T., Fukami, K., Thelen, M., Golub, T., Frey, D. & Caroni, P. (2000) GAP43, MARCKS, and CAP23 modulate PI(4,5)P(2) at plasmalemmal rafts, and regulate cell cortex actin dynamics through a common mechanism. *J. Cell Biol.*, **149**, 1455–1472.

Leshchyns'ka, I., Sytnyk, V., Morrow, J.S. & Schachner, M. (2003) Neural cell adhesion molecule (NCAM) association with PKC*β* via *β*1 spectrin is implicated in NCAM-mediated neurite outgrowth. *J. Cell Biol.*, **161**, 625–639.

Magill, C.K., Tong, A., Kawamura, D., Hayashi, A., Hunter, D.A., Parsadanian, A., Mackinnon, S.E. & Myckatyn, T.M. (2007) Reinnervation of the tibialis anterior following sciatic nerve crush injury: a confocal microscopic study in transgenic mice. *Exp. Neurol.*, **207**, 64–74.

Maness, P.F. & Schachner, M. (2007) Neural recognition molecules of the immunoglobulin superfamily: signaling transducers of axon guidance and neuronal migration. *Nat. Neurosci.*, **10**, 19–26.

Martini, R. & Schachner, M. (1986) Immunoelectron microscopic localization of neural cell adhesion molecules (L1, N-CAM, and MAG) and their shared carbohydrate epitope and myelin basic protein in developing sciatic nerve. *J. Cell Biol.*, **103**, 2439–2448.

Maselli, R.A., Wollman, R.L., Leung, C., Distad, B., Palombi, S., Richman, D.P., Salazar-Grueso, E.F. & Roos, R.P. (1993) Neuromuscular transmission in amyotrophic lateral sclerosis. *Muscle Nerve*, **16**, 1193–1203.

Meiri, K.F., Saffell, J.L., Walsh, F.S. & Doherty, P. (1998) Neurite outgrowth stimulated by neural cell adhesion molecules requires growth associated protein-43 (GAP-43) function and is associated with GAP-43 phosphorylation in growth cones. *J. Neurosci.*, **18**, 10429–10437.

Milner-Brown, H.S. & Stein, R.B. (1975) The relation between the surface electromyogram and muscular force. *J. Physiol.*, **246**, 549–569.

Miniou, P., Tiziano, D., Frugier, T., Roblot, N., Le Meur, M. & Melki, J. (1999) Gene targeting restricted to mouse striated muscle lineage. *Nucleic Acids Res.*, **27**, e27.

Moscoso, L.M., Cremer, H. & Sanes, J.R. (1998) Organization and reorganization of neuromuscular junctions in mice lacking neural cell adhesion molecule, tenascin-C, or fibroblast growth factor-5. *J. Neurosci.*, **18**, 1465–1477.

Neithammer, P., Delling, M., Sytnyk, V., Dityatev, A., Fukami, K. & Schachner, M. (2002) Cosignaling of NCAM via lipid rafts and the FGF receptor is required for neuritogenesis. *J. Cell Biol.*, **157**, 521–532.

Nieke, J. & Schachner, M. (1985) Expression of the neural cell adhesion molecules L1 and N-CAM and their common carbohydrate epitope L2/HNK-1 during development and after transection of the mouse sciatic nerve. *Differentiation*, **30**, 141–151.

Pielage, J., Fetter, R.D. & Davis, G.W. (2005) Presynaptic spectrin is essential for synapse stabilization. *Curr. Biol.*, **15**, 918–928.

Pollerberg, G.E., Burridge, K., Krebs, K.E., Goodman, S.R. & Schachner, M. (1987) The 180-kD component of the neural cell adhesion molecule N-CAM is involved in cell-cell contacts and cytoskeleton-membrane interactions. *Cell Tissue Res.*, **250**, 227–236.

Polo-Parada, L., Bose, C.M. & Landmesser, L.T. (2001) Alterations in transmission, vesicle dynamics, and transmitter release machinery at NCAM-deficient neuromuscular junctions. *Neuron*, **32**, 815–828.

Rafuse, V.F. & Gordon, T. (1996) Self-reinnervated cat medial gastrocnemius muscles. I. comparisons of the capacity for regenerating nerves to form enlarged motor units after extensive peripheral nerve injuries. *J. Neurophysiol.*, **75**, 268–281.

Rafuse, V.F. & Landmesser, L.T. (2000) The pattern of avian intramuscular nerve branching is determined by the innervating motoneuron and its level of polysialic acid. *J. Neurosci.*, **20**, 1056–1065.

Rafuse, V.F., Gordon, T. & Orozco, R. (1992) Proportional enlargement of motor units after partial denervation of cat triceps surae muscles. *J. Neurophysiol.*, **68**, 1261–1276.

Rafuse, V.F., Polo-Parada, L. & Landmesser, L.T. (2000) Structural and functional alterations of neuromuscular junctions in NCAM-deficient mice. *J. Neurosci.*, **20**, 6529–6539.

Reddy, L.V., Koirala, S., Sugiura, Y., Herrera, A.A. & Ko, C.-P. (2003) Glial cells maintain synaptic structure and function and promote development of the neuromuscular junction in vivo. *Neuron*, **40**, 563–580.

Redfern, P.A. (1970) Neuromuscular transmission in new-born rats. *J. Physiol.*, **209**, 701–709.

Reynolds, M.L. & Woolf, C.J. (1992) Terminal Schwann cells elaborate extensive processes following denervation of the motor endplate. *J. Neurocytol.*, **21**, 50–66.

Rich, M.M., Wang, X., Cope, T.C. & Pinter, M.J. (2002) Reduced neuromuscular quantal content with normal synaptic release time course and depression in canine motor neuron disease. *J. Neurophysiol.*, **88**, 3305–3314.

Rieger, F., Grumet, M. & Edelman, G.M. (1985) N-CAM at the vertebrate neuromuscular junction. *J. Cell Biol.*, **101**, 285–293.

Rieger, F., Nicolet, M., Picon-Raymond, M., Murawsky, M., Levi, G. & Edelman, G.M. (1988) Distribution and role in regeneration of N-CAM in the basal lamina of muscle and Schwann cells. *J. Cell. Biol.*, **107**, 707–719.

Robitaille, R. (1998) Modulation of synaptic efficacy and synaptic depression by glial cells at the frog neuromuscular junction. *Neuron*, **21**, 847–855.

Rochel, S. & Robbins, N. (1988) Effect of partial denervation and terminal field expansion on neuromuscular transmitter release and nerve terminal structure. *J. Neurosci.*, **8**, 332–338.

Sadasivam, G., Willmann, R., Lin, S., Erb-Vögtli, S., Kong, X.C., Rüegg, M.A. & Fuhrer, C. (2005) Src-family kinases stabilize the neuromuscular synapse in vivo via protein interactions, phosphorylation, and cytoskeletal linkage of acetylcholine receptors. *J. Neurosci.*, **25**, 10479–10493.

Schuster, C.M., Davis, G.W., Fetter, R.D. & Goodman, C.S. (1996) Genetic dissection of structural and functional components of synaptic plasticity. I. Fasciclin II controls synaptic stabilization and growth. *Neuron*, **17**, 641–654.

Smith, C.L., Mittaud, P., Prescott, E.D., Fuhrer, C. & Burden, S.J. (2001) Src, Fyn, and Yes are not required for neuromuscular synapse formation but are necessary for stabilization of agrin-induced clusters of acetylcholine receptors. *J. Neurosci.*, **21**, 3151–3160.

Son, Y.-J. & Thompson, W.J. (1995) Nerve sprouting in muscle is induced and guided by processes extended by Schwann cells. *Neuron*, **14**, 133–141.

Sytnyk, V., Leshchyns'ka, I., Dityatev, A. & Schachner, M. (2004) Trans-Golgi network delivery of synaptic proteins in synaptogenesis. *J. Cell Sci.*, **117**, 381–388.

Thompson, W. & Jansen, J.K. (1977) The extent of sprouting of remaining motor units in partly denervated immature and adult rat soleus muscle. *Neuroscience*, **2**, 523–535.

Totosy de Zepetnek, J.E., Gordon, T., Stein, R.B. & Zung, H.V. (1991) Comparison of force and EMG measures in normal and reinnervated tibialis anterior muscles of the rat. *Can. J. Physiol. Pharmacol.*, **69**, 1774–1783.

Warita, H., Murakami, T., Manabe, Y., Sato, K., Hayashi, T., Seki, T. & Abe, K. (2001) Induction of polysialic acid-neural cell adhesion molecule in surviving motoneurons of transgenic amyotrophic lateral sclerosis mice. *Neurosci. Lett.*, **300**, 75–78.

Witzemann, V., Schwartz, H., Koenen, M., Berberich, C., Villarroel, A., Wernig, A., Brenner, H.R. & Sakmann, B. (1996) Acetylecholine receptor ε-subunit deletion causes muscle weakness and atrophy in juvenile and adult mice. *Proc. Natl Acad. Sci. USA*, **93**, 13286–13291.

Woolf, C.J., Reynolds, M.L., Chong, M.S., Emson, P., Irwin, N. & Benowitz, L.I. (1992) Denervation of the motor endplate results in the rapid expression by terminal Schwann cells of the growth associated protein GAP-43. *J. Neurosci.*, **12**, 3999–4010.

Yang, J.F., Stein, R.B., Jhamandas, J. & Gordon, T. (1990) Motor unit numbers and contractile properties after spinal cord injury. *Ann. Neurol.*, **28**, 496–502.

Yang, X., Arber, S., William, C., Li, L., Tanabe, Y., Jessell, T.M., Birchmeier, C. & Burden, S. (2001) Patterning of muscle acetylcholine receptor gene expression in the absence of motor innervation. *Neuron*, **30**, 399–410.